Mon. Not. R. astr. Soc. (1981) **194**, 601–612

Investigation of the optical fields of flat-spectrum radio sources to faint limiting magnitudes

J. A. Peacock★, M. A.C. Perryman† and M. S. Longair★
Mullard Radio Astronomy Observatory, Cavendish Laboratory, Madingley Road, Cambridge CB3 0HE
J. E. Gunn and J. A. Westphal *The Hale Observatories, California Institute of Technology, Pasadena, California 91125, USA*

Received 1980 July 1

Summary. A deep optical survey of the fields of 16 flat-spectrum radio sources has been carried out using the Hale 5-m telescope, with a prototype charge-coupled device as a detector. These sources are members of a complete sample, selected as having $S(2.7\,\mathrm{GHz}) > 1.5$ Jy, and were either unidentified, or were identified with very faint objects on the prints of the Palomar Sky Survey.

Identifications are found for 12 of these objects; six are galaxies and six are stellar objects. Identifications for the 2.7-GHz sample are therefore now 96 per cent complete, allowing much improved redshift distributions to be derived. Values of $V/V_{\max}$ for the sample members have also been calculated, with the result that $\langle V/V_{\max}\rangle$ for the flat-spectrum quasars is 0.68, rather than the values nearer 0.5 derived from studies of deeper samples. This result indicates that both the steep-spectrum and flat-spectrum quasars undergo similar degrees of cosmological evolution.

1 Introduction

The 16 sources considered in this paper are taken from the complete sample of 168 sources described by Peacock & Wall (1981). This comprises the brightest sources in the northern sky at 2.7 GHz, selected according to the following criteria:

(1) $S_{2.7} \geqslant 1.5$ Jy on the Parkes flux-density scale,
(2) Dec $> 10°$,
(3) $|b| > 10°$.

★ Present address: Royal Observatory, Blackford Hill, Edinburgh EH9 3HJ.
† Present address: Astronomy Division, European Space Research and Technology Centre, Noordwijk, The Netherlands.

All of these sources have been observed with the Cambridge 5-km telescope at either 5 or 2.7 GHz with a resolution of 2 and 4 arcsec respectively.

This sample differs considerably from the analogous low-frequency samples (e.g. the 166-source 3CR sample of Jenkins, Pooley & Riley 1977); only about 50 per cent of the sources in the 2.7-GHz sample appear also in the 166-source sample. The new sources are those with flatter spectra, and those considered here belong to this group although, strictly speaking, seven of the sources in this paper are in fact steep-spectrum objects in that they have $\alpha_{2.7}^{5} \geqslant 0.5$. The terms steep-spectrum and flat-spectrum will be used in this precise sense hereafter. A striking feature of these new sources is that the majority of them are unresolved by the 5-km telescope; this is the case for 15 of the 16 sources considered here. Only 0411+14 is extended: it has a classical double structure with a weak central component. The identification statistics for the sample, divided into the various spectral and morphological classes, are given in Table 1. The optical classifications are as follows:

Q: Quasar. Confirmed by spectrum or variability (this class includes BL Lac objects).
Q?: Possible quasar – blue stellar object.
G: Galaxy. Confirmed by spectrum or by extended image.
G?: Possible galaxy – red stellar object.
EF: Empty field.
SO: Neutral stellar object.

In the remainder of this paper, we shall use the term 'quasar' for those sources classified as Q, Q? or SO, and 'galaxy' for those classified as G or G?. We see that unresolved and extended sources differ in that the former are mainly quasars, while the latter are mainly galaxies. The identifications for the extended sources were essentially complete before the investigations described here – there were only two empty fields, whereas for the unresolved sources there were 17 empty fields. The aim of the present observations was to examine 16 of this total of 19 empty fields more closely, in an attempt to raise the identification percentage for the unresolved sources to a level comparable with that for the extended sources. We expected such investigations to be successful for the following reasons:

(a) Since we are dealing with unfamiliar non-3CR sources, few of the optical fields have been examined to limiting magnitudes fainter than those of the Palomar Sky Survey (PSS) – i.e. magnitudes of 20 in the red and 21 in the blue.

Table 1. Identification statistics.

(a) Steep-spectrum sources.

	Q	Q?	SO	G	G?	EF	Total
Extended sources	9	0	0	68	2	1	80
Unresolved sources	14	4	1	10	4	4	37
Total	23	4	1	78	6	5	117
This paper	0	2	0	3	0	2	

(b) Flat-spectrum sources.

	Q	Q?	SO	G	G?	EF	Total
Extended sources	4	0	0	0	1	0	5
Unresolved sources	19	12	4	8	1	2	46
Total	23	12	4	8	2	2	51
This paper	1	3	0	3	0	2	

(b) Because we are dealing with mainly unresolved objects, the radio positions derived from the 5-km observations are very accurate (typical error < 0.5 arcsec), so ambiguous identifications can be avoided.

The observations, together with the data reduction procedures, are described in Section 2, and the identification procedure and results in Section 3. Estimation of magnitudes is discussed in Section 4, and Section 5 relates the results to the identification content of the whole sample.

2 Observations and data reduction

The observations were made on the nights of 1979 March 2 and 3 and 1979 October 17, together with observations of 3CR sources. The instrumentation and reduction procedure was the same in each case and will be described only briefly since a fuller description is given by Gunn *et al.* (1981).

The detector was a prototype charge-coupled device (CCD) with 500×500 picture elements (see Antcliffe 1975), mounted at the prime focus of the Hale 5-m telescope. A re-imaging system yielded a field of view 3.6 arcmin across. CCD detectors have many advantages over conventional photographic plates, in particular a high quantum efficiency (60 per cent in this case) and a response which is linear over a very wide dynamic range (4000 in this case). The filter used was the *r* filter from the photometric system of Wade *et al.* (1979). For each field the exposure was 5 min.

At the end of integration, the number of electrons in each pixel of the CCD was counted, providing a number proportional, in principle, to the number of photons received. However, these raw data suffer from certain defects:

(a) Near to bright stars, electrons may leak from pixel to pixel. This produces streaks on the image which are parallel to the direction in which the CCD data are read out (by moving the accumulated electrons along a line of pixels).

(b) There are lines of defective pixels on the CCD, which lead to light or dark streaks on the image in the same position for all fields.

(c) The response of each pixel is not the same; there may be variations in quantum efficiency and in dark current across the CCD.

(d) The CCD is subject to contamination by cosmic-ray showers, which can cause spurious images to appear on the CCD field. These effects are discussed by Gunn *et al.* (1981), but are not a problem here as the probability of one of these events occurring at the radio position is negligible.

Defect (c) is the most easily corrected: a series of test exposures both with zero and with uniform illumination were taken. These allow variations in sensitivity to be corrected. In practice, the dark current generation was found to be negligible and pixel-to-pixel variations in response were stable in time.

It is possible to correct for defect (b) by interpolation over the lines of defective pixels. Quite apart from improving the appearance of the final images, this is a necessary procedure in order to ensure that magnitudes of individual objects are not systematically in error due to the loss of signal in the affected areas.

3 Identification procedure

The position of the radio source on the CCD image was found by comparison with the positions of secondary standard stars which also appear on the CCD image. These latter were determined with respect to AGK3 stars by measurements of PSS prints using an x–y

measuring machine (*cf.* Laing *et al.* 1978). The main source of error in this process was the faintness of the secondary standards, which meant that accurate x–y coordinates were difficult to obtain. All reductions from the PSS were performed twice, inverting the print so as to eliminate any systematic error in setting on the faint objects. The resulting positions were usually within 1 arcsec of each other. By using prints of the CCD fields on an expanded scale, such problems were avoided, and the final errors in the derived positions are essentially the standard errors of fitting rectangular coordinates on the CCD plates to the secondary standard positions; these were typically < 1 arcsec.

The reliability of the candidate identifications was measured by the parameter R:

$$R = \left(\frac{(\Delta\alpha)^2}{\sigma_{\alpha o}^2 + \sigma_{\alpha R}^2} + \frac{(\Delta\delta)^2}{\sigma_{\delta o}^2 + \sigma_{\delta R}^2} \right)^{1/2},$$

where $\Delta\alpha$ and $\Delta\delta$ are the differences in radio and optical RA and Dec, and $\sigma_{\alpha o}$, $\sigma_{\alpha R}$, $\sigma_{\delta o}$ and $\sigma_{\delta R}$ are the RA and Dec errors in the optical and radio positions. R has the integral probability distribution

$$P(R > R_o) = \exp(-R_0^2/2)$$

(de Ruiter, Willis & Arp 1977) and the selection criterion was chosen to be $R = 3$, since there is only a 1 per cent probability that $R > 3$ for a genuine identification.

Application of this procedure yielded 12 identifications. These are presented in Plates 1 and 2: Plate 1 gives finding photographs 15 arcmin square taken from the red PSS prints, with the area of the CCD field shown; Plate 2 presents the CCD fields as 'Photowrite' plates 3.2 arcmin square, on which the density scale is linearly proportional to intensity over the range 0.5 σ to 10σ above the background, where σ is the noise level at the radio position. Identifications are indicated by a pair of lines, and empty fields by a circle of radius 10 arcsec. In six cases it is obvious whether the object is stellar or extended (0026+34, 0404+76, 0411+14, 0710+43, 0814+42 and 1358+62). The other six are all faint and require further examination. Fig. 1 shows intensity profiles through these six objects, together with

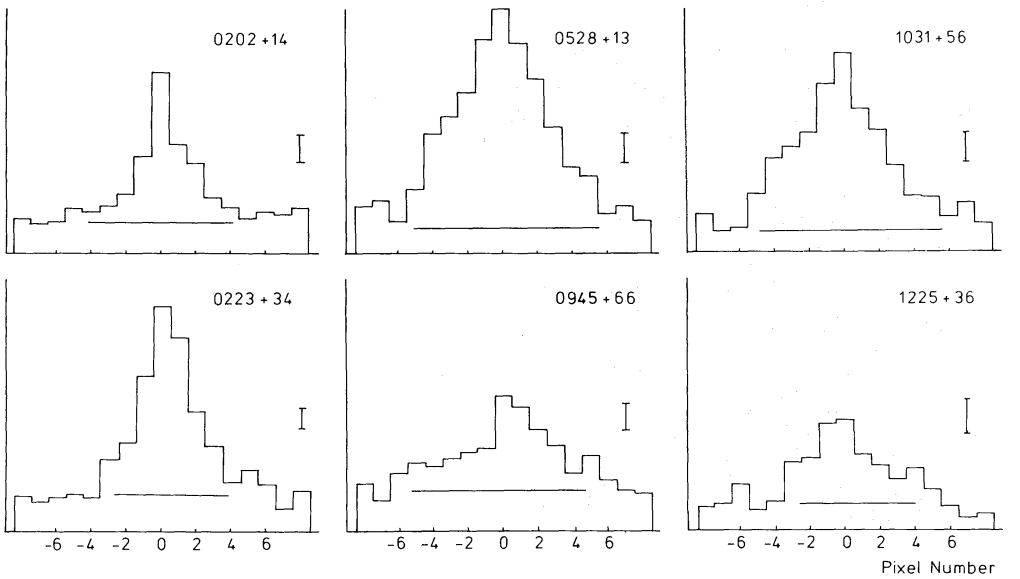

Figure 1. Plots of intensity profiles for the six faintest identifications. Intensity in arbitrary units is plotted against pixel number. The horizontal line indicates the background level and the error bar indicates the noise level.

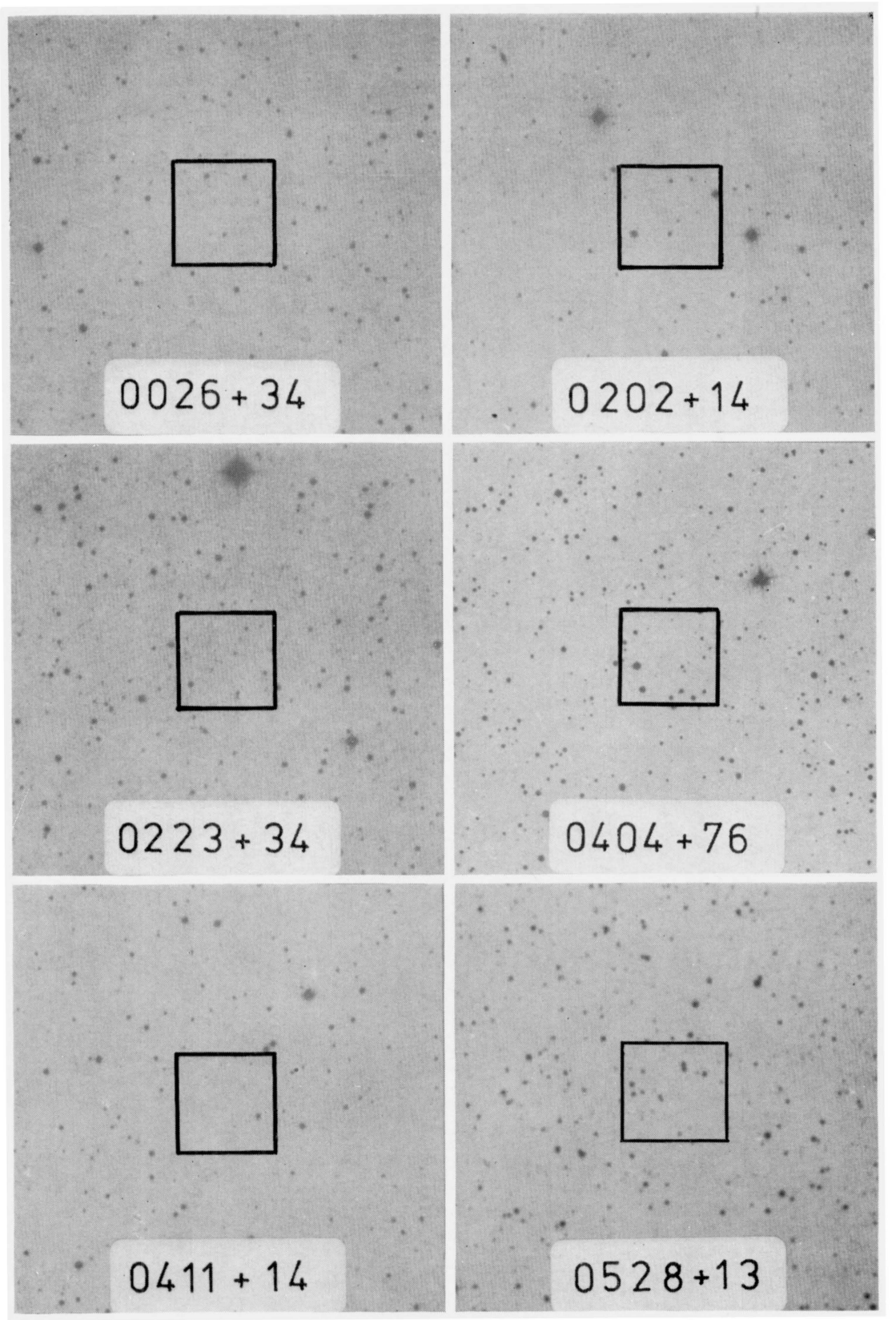

Plate 1. Finding photographs for the radio-source fields. These are taken from the E plates of the PSS (copyright by the National Geographic Society–Palomar Observatory sky survey. Reproduced by permission of the Hale Observatories). Each photograph is 15 arcmin square, with north to the top and east to the left. The central square shows the area of the CCD plate.

[*facing page* 604]

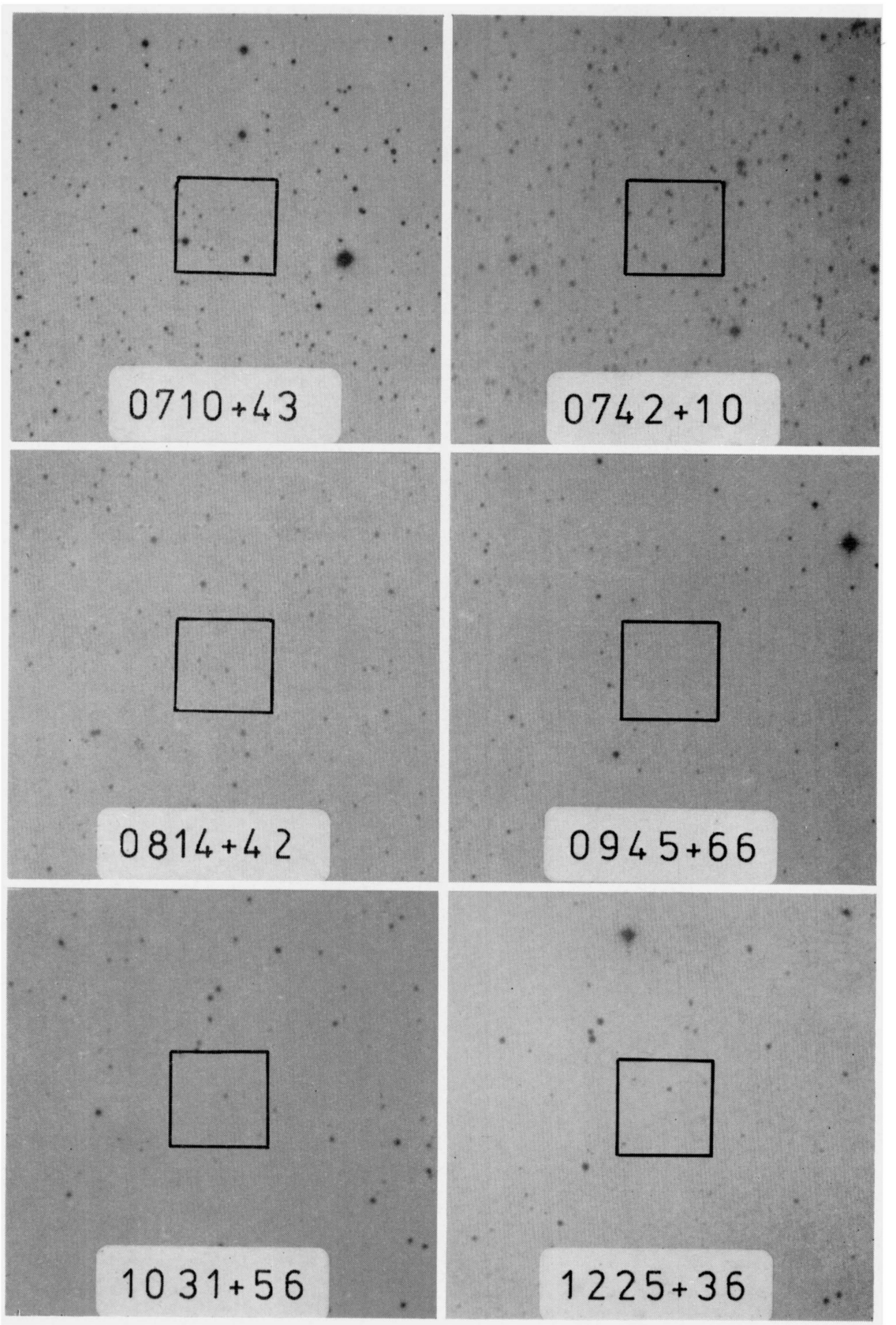

Plate 1.—*continued*

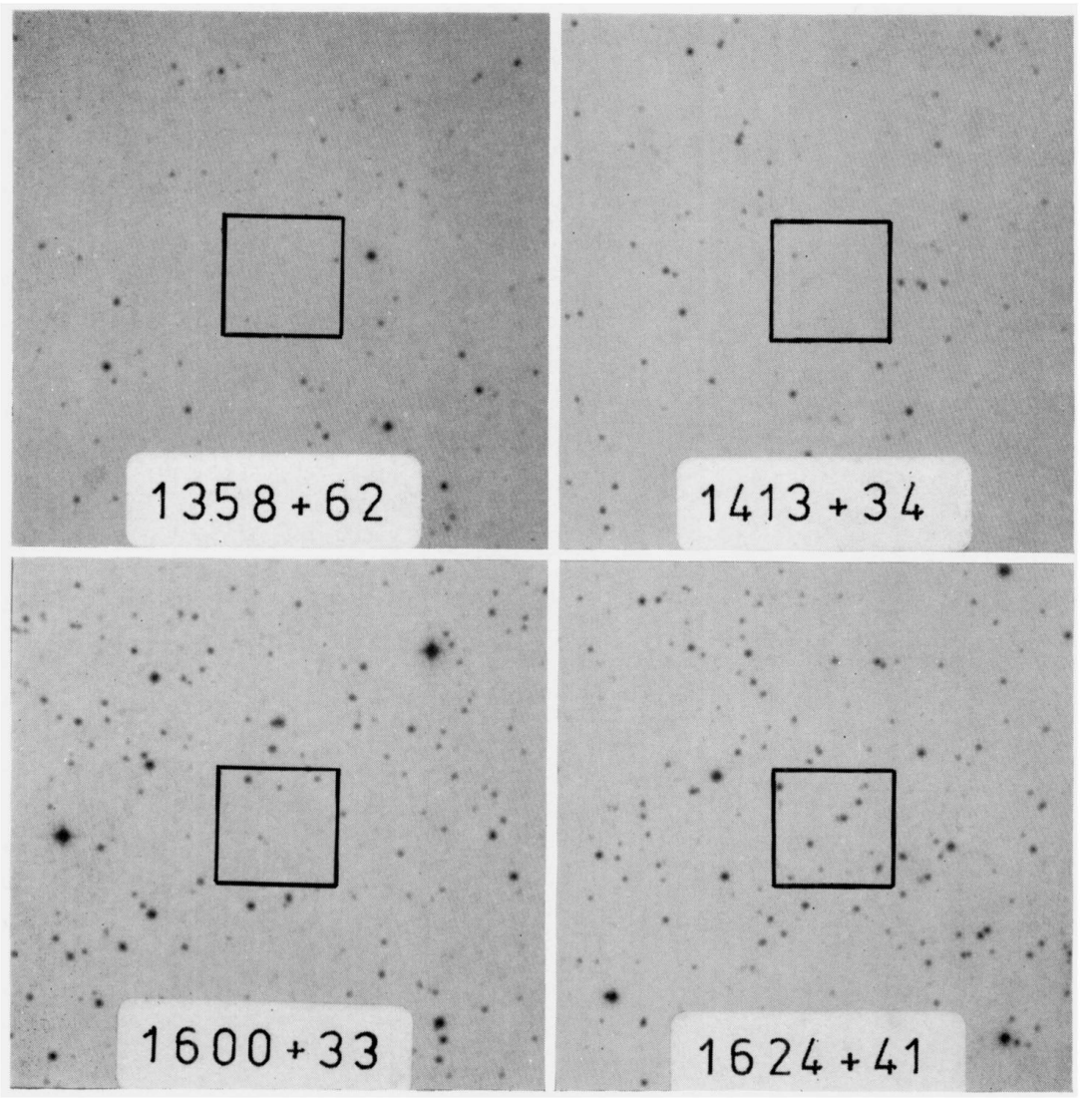

Plate 1.—*continued*

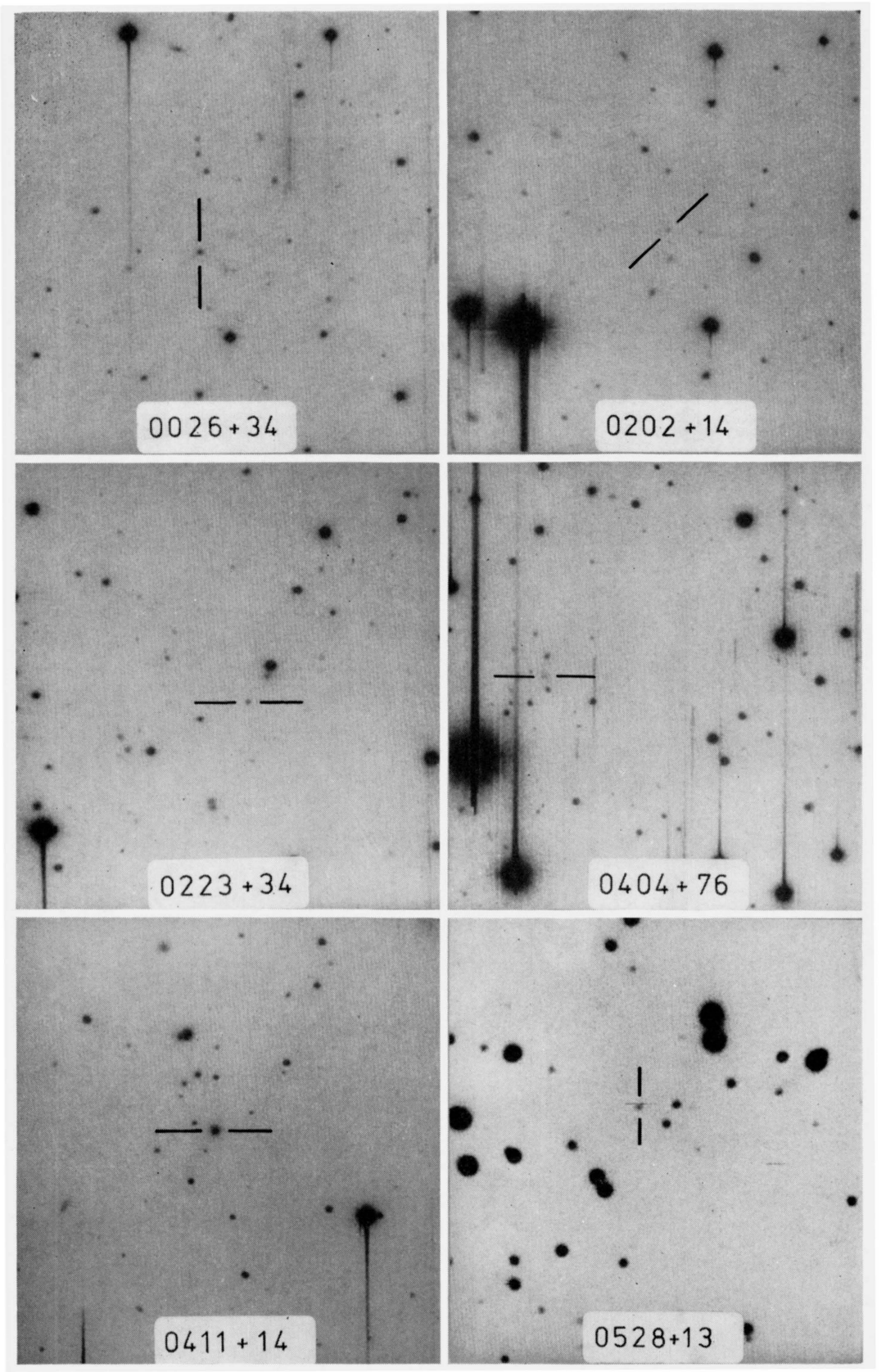

Plate 2. The photowrite images of the CCD fields. These are 450 pixels (3.2 arcmin) square, with north to the top and east to the left. The positions of the identifications are indicated by a pair of lines. In the case of the empty fields, a circle of radius 10 arcsec is drawn at the radio position.

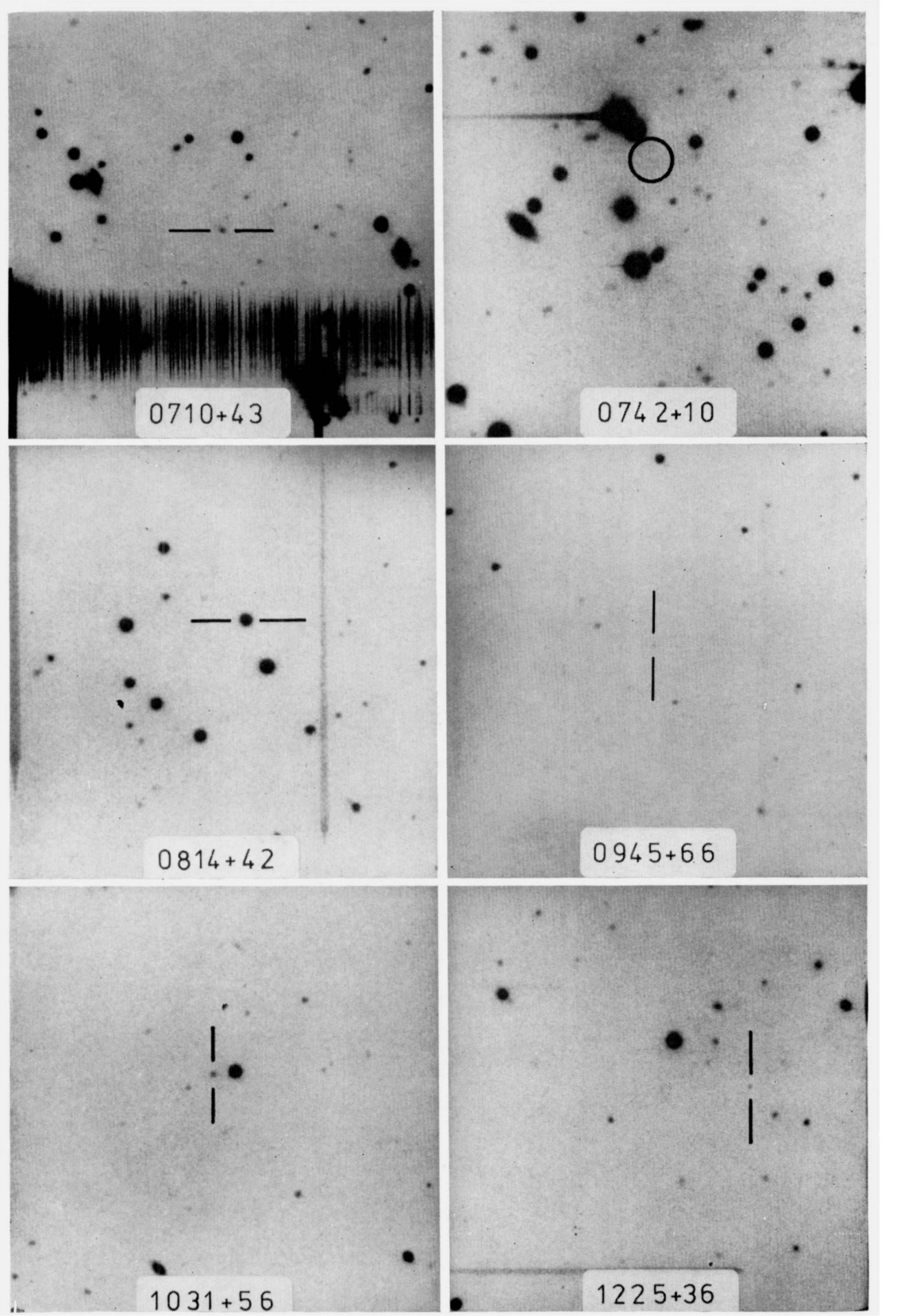

Plate 2.—*continued*

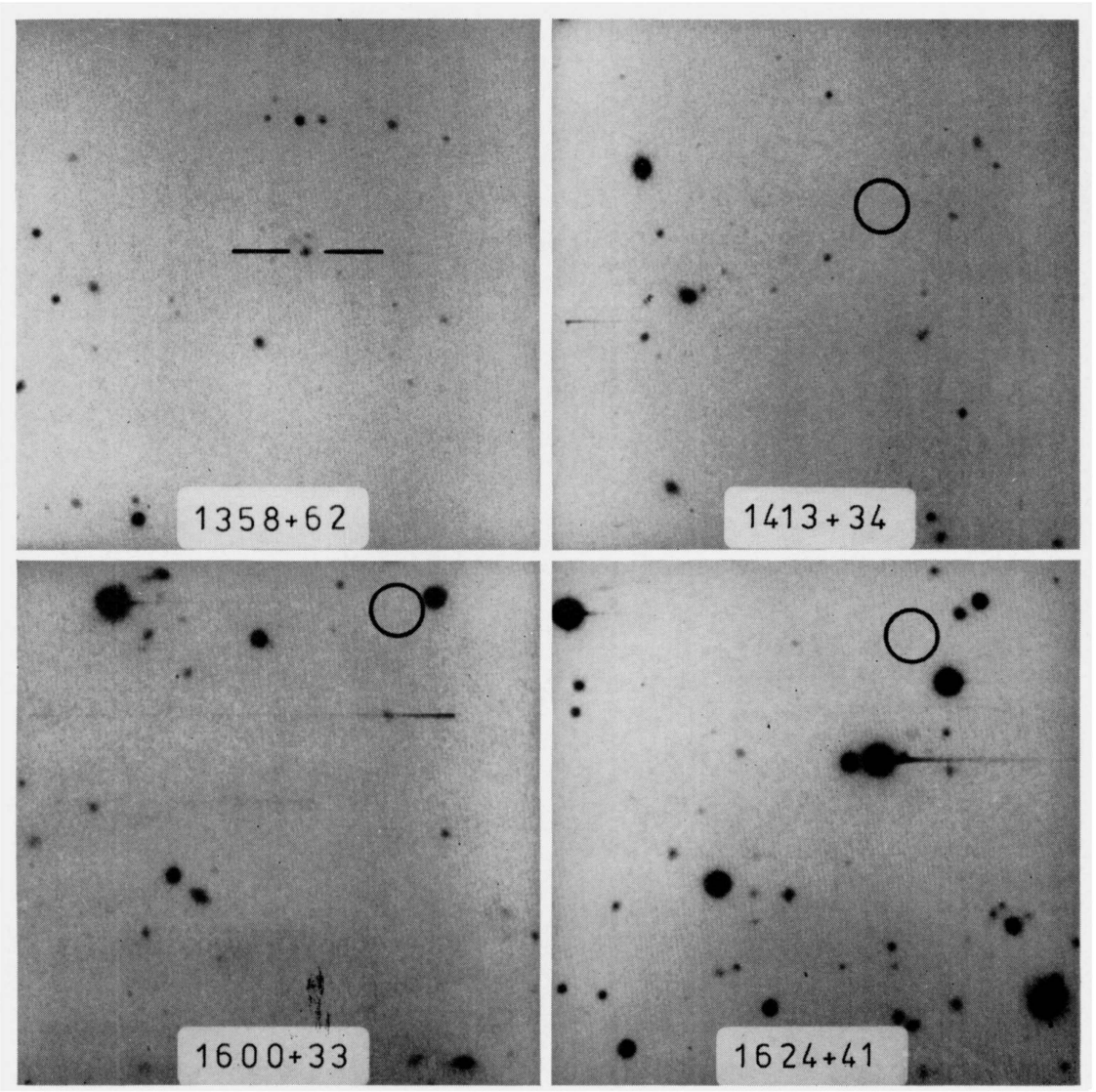

Plate 2.—*continued*

Table 2. Summary of results.

(1)	(2)	(3)	(4)	(5)	(6)	(7)	(8)	(9)
0026+34	OB343	00 26 34.81	34 39 57.8	0.06	-0.9	G	20.2	0.1
0202+14	4C15.05	02 02 07.40	14 59 51.3	0.03	0.7	SO	21.9	0.2
0223+34	4C34.07	02 23 09.72	34 08 01.3	0.03	-1.4	SO	21.3	0.1
0404+76	4C76.03	04 04 00.13	76 48 52.5	0.93	0.2	G	21.0	0.2
0411+14	4C14.11	04 11 40.94	14 08 48.3	0.03	5.2	G	19.1	0.1
0528+13	OG147	05 28 06.73	13 29 41.9	0.00	0.3	SO	20.3	0.2
0710+43	OI147	07 10 03.33	43 54 26.1	0.00	-0.1	G	19.7	0.2
0742+10	OI471	07 42 48.45	10 18 32.4	-	-	EF	-	-
0814+42	OJ425	08 14 51.67	42 32 07.7	0.01	-0.2	SO	17.7	0.1
0945+66	4C66.09	09 45 14.93	66 28 59.1	0.09	-0.1	G	21.6	0.5
1031+56	OL553	10 31 56.00	56 44 18.1	-0.03	0.2	SO	20.3	0.1
1225+36	ON343	12 25 30.79	36 51 47.1	0.11	1.5	SO	21.7	0.2
1358+62	4C62.22	13 58 58.30	62 25 08.4	0.13	-0.2	G	19.9	0.2
1413+34	OQ323	14 13 56.29	34 58 29.5	-	-	EF	-	-
1600+33	OS300	16 00 11.94	33 35 09.6	-	-	EF	-	-
1624+41	4C41.32	16 24 18.21	41 41 23.2	-	-	EF	-	-

the mean background level and the noise level for each source. Five of the objects have profiles which are apparently unresolved, but the sixth (0945+66) seems to show a halo above the noise.

The details of these identifications are summarized in Table 2 as follows:

(1) IAU – type name;
(2) Other name;
(3) Radio RA (1950.0);
(4) Radio Dec (1950.0);
(5) Optical RA – Radio RA in s;
(6) Optical Dec – Radio Dec in arcsec;
(7) Optical classification: G (galaxy) if extended, otherwise SO (stellar object);
(8) *r* magnitude (see Section 4);
(9) Formal error in *r* magnitude (see Section 4).

NOTES ON INDIVIDUAL SOURCES

0710+43

The 19.7-mag galaxy is visible on the PSS as a very faint object just above the plate limit, but it is impossible to say from this whether it is extended. This image shows several of the spurious cosmic-ray events referred to in Section 2.

0814+42

The stellar object detected here is visible on the PSS as a faint object of red magnitude about 19. The measured magnitude of 17.7 on the CCD field is much brighter than this, providing

definite evidence for variability over the period 1955–1979 (and therefore confirming the identification as a QSO). In fact, it is obvious from Plates 1 and 2 that the object has brightened relative to its neighbours.

1358+62

The 19.9-mag galaxy is visible on the PSS (E plate only) as a very faint object. Again, no information beyond the bare detection can be derived from the image.

Finally, we must consider the probability that these identifications are chance coincidences. In fact, due to the high accuracy of both the radio and optical positions, this is relatively unlikely. The most heavily populated CCD field is that of 0742+10 which contains 62 objects on the image shown in Plate 2; this corresponds to a density of 0.0017 arcsec^{-2}. For a small radio positional error, $R = 3$ corresponds to a circle of radius 2.1 arcsec, so there is a probability of only 2 per cent that a background object will lie within our search area by chance. This calculation assumes that the objects are scattered at random on the plate – which is not the case. Nevertheless, the degree of clustering is not large and the majority of the fields are much less dense than that of 0742+10, so these effects will generally be negligible.

4 Estimation of magnitudes

The estimation of magnitudes is, in principle, simplified by the linearity of the CCD; the data (after correction for the defects described in Section 2) provide a signal which is directly proportional to the photon count across the field. However, before these counts can be integrated to find the magnitudes of individual objects, a correction must be made for the effects of the sky background, which dominates the signal for the fainter objects considered here. The level of this background may be determined by integration of the photon counts in empty regions of the sky surrounding the source, allowing the effects of the background to be subtracted from the integrated counts for individual objects. There remains the question of the integration area to be used; for stellar objects there is no difficulty, but for E galaxies there is an uncertainty. If the redshifts of the galaxies were known and a world model assumed, it would be possible to measure the light within a fixed physical dimension at the galaxy, for example a radius of 16 kpc as used by Gunn & Oke (1975) in their study of the redshift–magnitude relation. Since the redshifts are not known, we have adopted instead the cruder procedure of measuring the total magnitude of the galaxy within an area 9 arcsec square (i.e. 20 x 20 pixels). If the redshifts of the galaxies lie in the range 0.5–1.0, then the size of this square corresponds to 50–100 kpc, and a large fraction of the light of the galaxies will be included. In view of the problems mentioned above, it is not worth attempting a better determination of the apparent magnitudes at this stage.

To calibrate these photon counts to an absolute photometric scale, two of the standard stars of Wade *et al.* (1979) (HD 84937 and DM+262606) were observed and reduced as above. This process yields the r magnitudes given in Table 2. The quoted formal errors of about 0.2 mag are mainly due to uncertainties in the background removal. In individual cases the real errors may be higher, due either to perverse background variations (e.g. a local 'hole' at the source position) or to problems with the integration area. The magnitudes should still, however, be accurate to better than 0.5 mag, at least for the stellar objects.

5 Discussion

The results of the present survey enable us for the first time to obtain a more-or-less complete picture of the radio source population selected at high frequencies and high flux density. Of

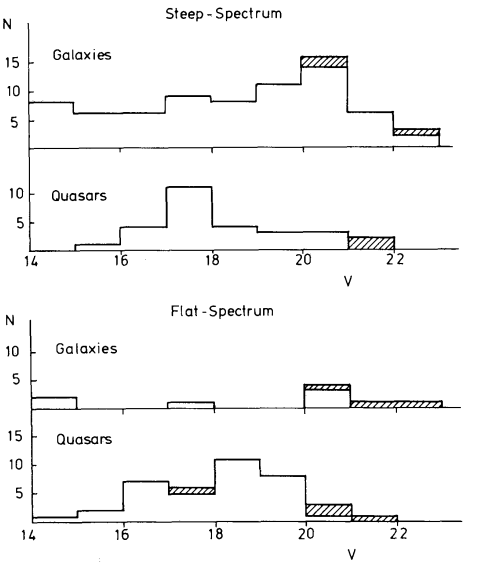

Figure 2. Distributions of V magnitudes for the sources in the 2.7-GHz sample, divided into quasars and galaxies of each spectral type. The data from the present paper are shown hatched.

the 168 sources in the sample, only one of the extended sources and six of the compact sources remain unidentified. The present sample is the high-frequency analogue of the statistical sample of 166 3CR sources (see Jenkins *et al.* 1977; Gunn *et al.* 1981), and the details of the statistics shown in Table 1 indicate the differences in the samples selected at low and high frequencies. We can quantify these differences in a number of ways:

Fig. 2 shows the V-magnitude distributions for the sample, divided into galaxies and quasars of each spectral type. The hatched boxes indicate the newly identified sources; the r magnitudes given here have been converted to V magnitudes by assuming the relations $V-R=1$ for galaxies and $V-R=0$ for quasars. The histograms for the steep-spectrum sources are similar to the distributions found in low-frequency samples. As is well-known, virtually all the new identifications found in deep optical surveys of samples selected at low radio frequencies (e.g. Gunn *et al.* 1981) are with faint galaxies and there are very few quasars with $V<20$. In contrast, our new identifications include five quasars with $20<r<22$ – two of which are steep-spectrum, although the proportion of steep-spectrum sources in this sample with $V>20$ which are quasars is still very small.

Fig. 3 shows the redshift distributions for the steep- and flat-spectrum sources. Redshifts have been estimated for those sources without measured values by using the redshift–magnitude relations for galaxies and quasars separately. These estimates are rough, particularly for the quasars, but the general shapes of the distributions should nevertheless be well defined. Unidentified sources have been given a redshift $z=1$ to indicate how little difference their true redshifts will make to the overall shape of the distributions.

As expected, the flat-spectrum sub-sample is more strongly biased towards large redshifts than is the steep-spectrum sub-sample, since the former class contains a much larger proportion of quasars. It is of importance that, considering the quasars alone, there is no evidence for any difference in redshift distributions for the two spectral types. Thus, if the steep-spectrum and flat-spectrum quasars show differences in their evolutionary behaviours, these must be attributed to physical differences in the evolution, rather than to differences in the redshift ranges spanned.

To find out if this is the case for the present sample, we used the redshift information to determine values of radio-limited $V/V_{\max}$ for the sample members. Since the sample is so

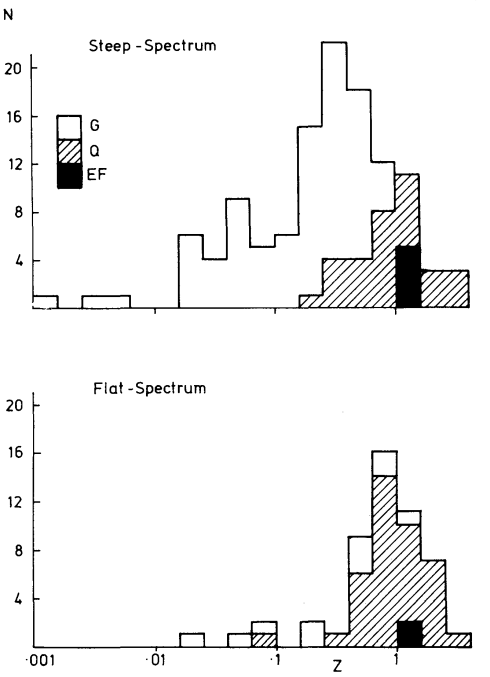

Figure 3. The redshift distributions for the 2.7-GHz sample, divided into the steep-spectrum and flat-spectrum classes.

close to being completely identified, the difference in V/V_{max} due to the assumption of an infinite magnitude limit rather than the true value of about $V = 22$ is negligible. Figs 4 and 5 show V/V_{max} plotted against luminosity (assuming $H_0 = 50\,km\,s^{-1}\,Mpc^{-1}$ and $q_0 = 0$) for the steep- and flat-spectrum sub-samples respectively. There are seen to be more sources with $V/V_{max} > 0.5$ for the flat-spectrum sample than for the steep-spectrum sample. The latter sample, however, contains a much larger fraction of sources with small redshifts. To make a

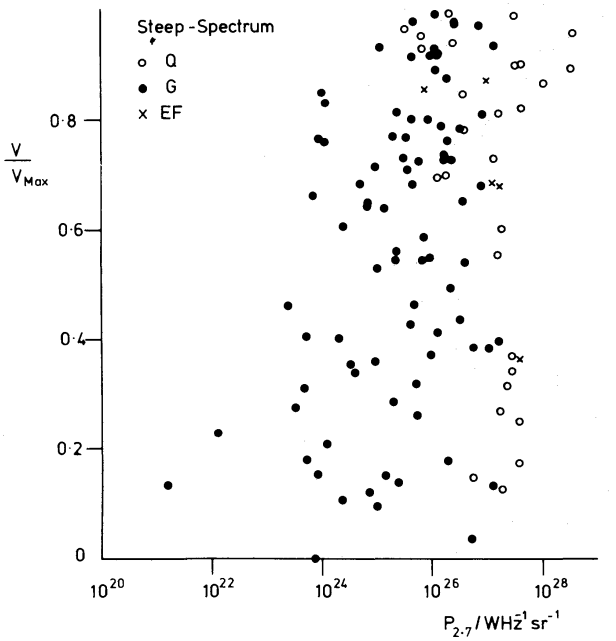

Figure 4. A plot of radio-limited V/V_{max} against luminosity for the steep-spectrum sources in the 2.7-GHz sample.

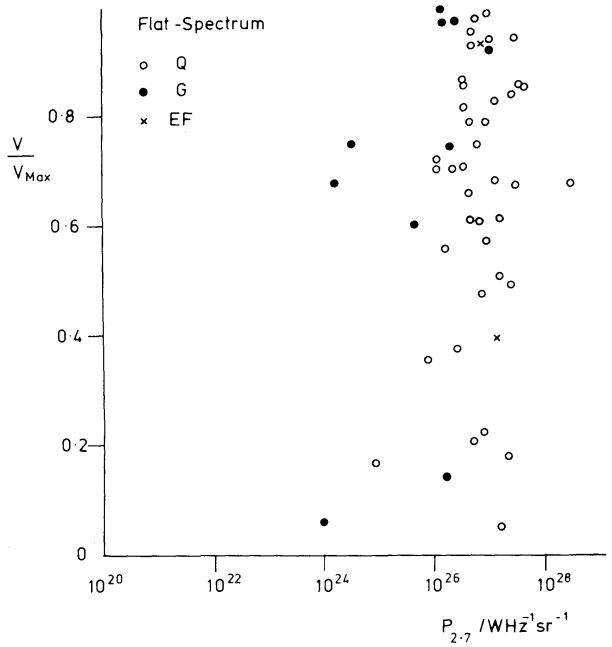

Figure 5. A plot of radio limited V/V_{max} against luminosity for the flat-spectrum sources in the 2.7-GHz sample.

proper comparison, we compare the values of $\langle V/V_{max}\rangle$ for sources with $P_{2.7} > 10^{26}$ and $< 10^{26}\,W\,Hz^{-1}\,sr^{-1}$ for both classes of source, and also for quasars alone (Table 3). In both cases, the low-luminosity sources have $\langle V/V_{max}\rangle$ consistent with a uniform distribution ($\langle V/V_{max}\rangle = 0.5$). The big surprises are the values of $\langle V/V_{max}\rangle$ for the steep-spectrum and flat-spectrum quasars, and for all sources with $P_{2.7} > 10^{26}\,W\,Hz^{-1}\,sr^{-1}$; these are all in the range 0.64 to 0.7. Remarkably, the largest values are associated with the flat-spectrum sources, in apparent contradiction with the results of previous workers who have studied the V/V_{max} test for flat-spectrum quasars.

The values of $\langle V/V_{max}\rangle$ for the steep-spectrum sources agree reasonably well with the results of Masson & Wall (1976, MW), $\langle V/V_{max}\rangle = 0.68 \pm 0.07$, and Wills & Lynds (1978, WL), $\langle V/V_{max}\rangle = 0.76 \pm 0.05$, but both sets of authors find significantly smaller values for the flat-spectrum quasars, $\langle V/V_{max}\rangle = 0.54 \pm 0.05$ and 0.61 ± 0.05 respectively. WL discuss the differences between these two analyses which consider essentially the identical set of flat-spectrum quasars, and favour a compromise value of about 0.6.

It may be argued that, given the statistical errors on these values, there is no compelling evidence for any difference in the $\langle V/V_{max}\rangle$ values for the steep-spectrum and flat-spectrum

Table 3. Values of $\langle V/V_{max}\rangle$.

(a) Steep-spectrum sources	
$P_{2.7} > 10^{26}\,W\,Hz^{-1}\,sr^{-1}$	0.661 ± 0.036
$P_{2.7} < 10^{26}\,W\,Hz^{-1}\,sr^{-1}$	0.536 ± 0.035
Quasars	0.640 ± 0.058
(b) Flat-spectrum sources	
$P_{2.7} > 10^{26}\,W\,Hz^{-1}\,sr^{-1}$	0.690 ± 0.037
$P_{2.7} < 10^{26}\,W\,Hz^{-1}\,sr^{-1}$	0.436 ± 0.106
Quasars	0.675 ± 0.038

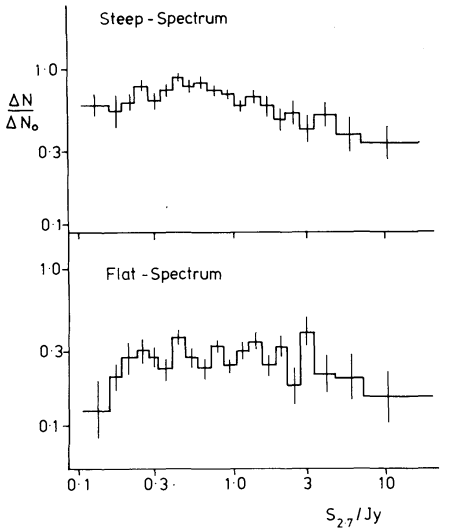

Figure 6. The differential source counts at 2.7 GHz, divided into the steep-spectrum and flat-spectrum classes. These counts are taken from Wall *et al.* (1980a) and are normalized to the Euclidean prediction $N_0 = 100\,(S_{2.7}/\mathrm{Jy})^{-3/2}$.

sources, but studies of the source counts confirm the reality of the difference. The point of importance is that the sample of sources studied by MW and WL was selected according to the criterion $S_{2.7} \geqslant 0.35$ Jy, whereas our sample refers to $S_{2.7} \geqslant 1.5$ Jy, i.e. a flux-density limit larger by a factor of 4. The source counts for steep-spectrum and flat-spectrum sources, derived from much larger samples of sources were constructed by Wall, Pearson & Longair (1981) and are reproduced in Fig. 6. There is a close relation between the slope of the source counts and the value of $\langle V/V_{\max}\rangle$ (e.g. Longair & Scheuer 1970), and it can be seen that the normalized differential source counts for the steep-spectrum sources are steeper than the Euclidean prediction throughout the flux density range $S_{2.7} \geqslant 0.3$ Jy, with roughly constant slope. Hence it is reasonable that the values of $\langle V/V_{\max}\rangle$ found at $S_{2.7} = 0.35$ Jy and 1.5 Jy should be similar. On the other hand, the source counts for the flat-spectrum sources are steeper than the Euclidean prediction for $S_{2.7} > 1$ Jy, but follow closely the Euclidean prediction for $0.3 < S_{2.7} < 1$ Jy. The $\langle V/V_{\max}\rangle$ values at $S_{2.7} = 1.5$ Jy are thus expected to be similar to those for the steep-spectrum sources, whereas the values of $\langle V/V_{\max}\rangle$ at $S_{2.7} = 0.35$ Jy should be significantly smaller, as is indeed found to be so. Notice that this result is based on samples much larger than those on which the $V/V_{\max}$ test has been performed. High values of $\langle V/V_{\max}\rangle$ were also found by Blake (1978), for a sample of bright, flat-spectrum quasars selected at 1400 MHz.

We therefore believe in the reality of the difference in the values of $\langle V/V_{\max}\rangle$ for flat-spectrum sources with $S_{2.7} \geqslant 1.5$ Jy and $S_{2.7} \geqslant 0.35$ Jy. The point of particular importance is that there exists a class of flat-spectrum sources for which the cosmological evolution is just as strong as that for powerful steep-spectrum sources. The obvious interpretation of this result is that the evolutionary behaviour is a strong function of radio luminosity for the flat-spectrum sources, and such a correlation is evident in Fig. 5. We note that a variation of evolution with radio luminosity is also necessary to explain the total counts of radio sources (see e.g. Wall, Pearson & Longair 1980).

Finally, we display the luminosity distributions for the complete samples in Fig. 7. It is striking that the luminosity distribution for the steep-spectrum sources is significantly broader than that found at 178 MHz (see e.g. Gunn *et al.* 1981). This can be entirely attributed to the correlation between radio luminosity and spectral index, which is in the sense that the most luminous sources have steeper spectra (see e.g. Laing & Peacock 1980).

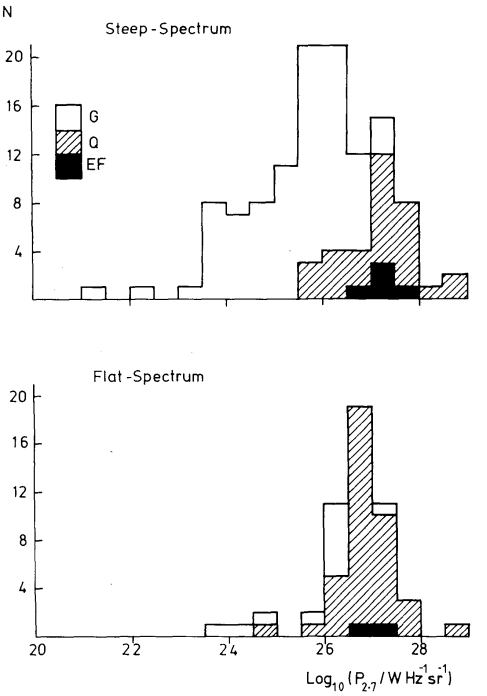

Figure 7. The luminosity distributions for the 2.7-GHz sample, divided into the steep-spectrum and flat-spectrum classes.

The luminosity distribution for the flat-spectrum sources is dominated by high-luminosity quasars. The rest of the distribution is rather poorly defined by the small number of flat-spectrum radio galaxies with low redshifts which appear in the sample. The observations described in this paper have allowed a much improved determination of these distributions, which provide essential information to constrain models of cosmological evolution at high frequencies (Peacock & Gull, in preparation). The main priority now is the determination of redshifts for the 42 identified sources for which these are still lacking, especially for the 24 quasars without redshifts. Nevertheless, the form of the luminosity distributions is unlikely to undergo any major change.

Acknowledgments

We thank M. A. Carr, R. Lucinio, V. E. Nanow and J. D. Smith for indispensable aid in the construction of the instrument; the Director of the Institute of Astronomy, Cambridge, for the use of their $x-y$ measuring machine; D. M. Odell, D. J. Titterington and P. J. Warner for help with the data reduction; and W. O. Saxton for the use of the Photowrite machine. We thank the Director of the Hale Observatories for observing privileges on the 5-m telescope, and we are very grateful to members of the Wide Field Camera Team of the Space Telescope Project for permission to use their CCD detector for these observations. JAP and MACP thank the SRC for financial support.

References

Antcliffe, G. A., 1975. *Texas Instruments Report 08-75-41.*
Blake, G. M., 1978. *Mon. Not. R. astr. Soc.*, **183**, 21P.
de Ruiter, H. R., Willis, A. G. & Arp, H. C., 1977. *Astr. Astrophys. Suppl.*, **28**, 211.
Gunn, J. E., Hoessel, J. G., Westphal, J. A., Perryman, M. A. C. & Longair, M. S., 1981. *Mon. Not. R. astr. Soc.*, **194**, 111.

Gunn, J. E. & Oke, J. B., 1975. *Astrophys. J.*, **195**, 255.
Jenkins, C. J., Pooley, G. G. & Riley, J. M., 1977. *Mem. R. astr. Soc.*, **84**, 61.
Laing, R. A., Longair, M. S., Riley, J. M., Kibblewhite, E. J. & Gunn, J. E., 1978. *Mon. Not. R. astr. Soc.*, **183**, 547.
Laing, R. A. & Peacock, J. A., 1980. *Mon. Not. R. astr. Soc.*, **190**, 903.
Longair, M. S. & Scheuer, P. A. G., 1970. *Mon. Not. R. astr. Soc.*, **151**, 45.
Masson, C. R. & Wall, J. V., 1977. *Mon. Not. R. astr. Soc.*, **180**, 193.
Peacock, J. A. & Wall, J. V., 1981. *Mon. Not. R. astr. Soc.*, **194**, 311.
Wade, R. W., Hoessel, J. G., Elias, J. H. & Huchra, J. P., 1979. *Publs astr. Soc. Pacif.*, **91**, 35.
Wall, J. V., Pearson, T. J. & Longair, M. S., 1980. *Mon. Not. R. astr. Soc.*, **193**, 683.
Wall, J. V., Pearson, T. J. & Longair, M. S., 1981. *Mon. Not. R. astr. Soc.*, in press.
Wills, D. & Lynds, R., 1978. *Astrophys. J. Suppl.*, **36**, 317.